

# Evaluation of hepatic fibrosis by ultrasonic acoustic structure quantification

Lei Cheng, MM<sup>a</sup>, Yongan Chen, MD<sup>b</sup>, Rui Xiao, PhD<sup>c</sup>, Yan Pan, MM<sup>d</sup>, Jia Guo, MD<sup>e,\*</sup>

## Abstract

To evaluate the diagnostic accuracy of ultrasonic acoustic structure quantification (ASQ) for grading hepatic fibrosis/cirrhosis by comparing ultrasonographic features of regions of interest on ASQ images with the pathological characteristics of stage F0–F4 hepatic fibrosis cases.

We retrospectively analyzed the medical records of 97 patients with chronic hepatitis who underwent ASQ evaluation at the Ultrasound Room of Dongfang Hepatobiliary Surgery Hospital (Shanghai, China) between July 2012 and October 2013. Regions of interest on stored ASQ images were analyzed to obtain cm<sup>2</sup> values on modes, averages, and standard deviations. Correlation analysis, principal component analysis (PCA), and multivariate analysis of variance (MANOVA) of the mean cm<sup>2</sup> values with hepatic fibrosis staging were performed. A receiver operating characteristic (ROC) curve was used to assess the diagnostic accuracy of ASQ.

The mean cm<sup>2</sup> of ASQ correlated with the pathological stage of hepatic fibrosis, with the best correlation coefficient ( $r = 0.81$ ) in the right lobe below rib 2. The best cm<sup>2</sup> average 1 and 2 values, which differed significantly among different hepatic fibrosis/cirrhosis stages, were also found in this area. The maximal area under the ROC curve (0.969) was for cm<sup>2</sup> average 1 for the F0 versus F1 to F4 group, with a low criterion (110), while the maximal criterion (145) was for cm<sup>2</sup> average 2 for the F0–F3 versus F4 group, with a relatively small AUC (0.882).

With objective and accurate results, ASQ analysis is a promising non-invasive method for grading hepatic fibrosis, although this should be verified in further studies.

**Abbreviations:** ALT = alanine aminotransferase, ASQ = acoustic structure quantification, AST = aspartate aminotransferase, AUROC = area under the ROC curve, CI = confidence interval, MANOVA = multivariate analysis of variance, PCA = principal component analysis, ROC = receiver operating characteristic, ROI = region of interest.

**Keywords:** acoustic structure quantification, hepatic fibrosis, ultrasonic elastography

## 1. Introduction

Hepatic fibrosis is marked by excessive deposition of extracellular matrix collagen, leading to degeneration, inflammation, and necrosis of the hepatic tissue.<sup>[1]</sup> Multiple cell types including TNF- $\alpha$ -producing NKp44+ NK cells<sup>[2]</sup> and multiple cellular proteins including heat shock protein 47 (HSP47)<sup>[3]</sup> are intimately implicated in hepatic fibrosis. While early hepatic

fibrosis is a reversible process, cirrhosis involves an irreversible lesion. Thus, early accurate diagnosis and treatment of hepatic fibrosis may effectively eliminate the cause of the disease, and delay or reverse the development of fibrosis.<sup>[4]</sup>

Liver biopsy has been the gold standard for the diagnosis of hepatic fibrosis and cirrhosis; however, liver biopsy is contraindicated in many conditions, including hepatic biliary tract obstruction, bacterial biliary tract infection, or biliary tract hemorrhage.<sup>[5,6]</sup> Moreover, since liver biopsy is an invasive procedure, it may cause subdiaphragmatic abscess, subcutaneous emphysema, pneumo-peritoneum, and other complications. Besides, most patients are unwilling to undergo liver biopsy. On the other hand, liver biopsy specimens are usually small, which may lead to an incorrect pathological diagnosis due to sampling bias.<sup>[7]</sup> Thus, liver biopsy is not undertaken routinely for the diagnosis of hepatic fibrosis and cirrhosis.

Ultrasound examination is non-invasive, involves no radiation and has no clinical contraindications. Conventional 2-dimensional ultrasonography can be used to evaluate diffuse liver lesions as well as morphological changes of the hepatic vein by assessing echo changes in the parenchyma.

Acoustic structure quantification (ASQ) is a new ultrasonographic technique that analyzes the intensity of echo signals in liver tissue as well as back-scattering changes.<sup>[8,9]</sup> ASQ quantitatively analyzes the difference in echo strength of the normal liver tissue against the echo strength of a region of interest (ROI) via secondary Chi-square analysis. Based on the images obtained from conventional ultrasonography, cm<sup>2</sup> (cm<sup>2</sup> = variance of actual measurements/normal liver variance) of mode, average, SD, and the RB ratio [the ratio of the area under the blue

Editor: Michael Masoomi.

LC and YC contributed equally to this manuscript.

All the authors declare that they have no conflict of interest.

Supplemental Digital Content is available for this article.

<sup>a</sup> Department of Echocardiography, Huashan Hospital, Fudan University,

<sup>b</sup> Department of Oncology, The 455th Hospital of Chinese People's Liberation Army, Shanghai, China, <sup>c</sup> Department of Anesthesiology, Columbia University Medical Center, New York, NY, <sup>d</sup> Department of Ultrasound, Yu Huang Ding Hospital, Yan Tai, <sup>e</sup> Department of Ultrasound, Eastern Hepatobiliary Surgery Hospital, Shanghai, China.

\* Correspondence: Jia Guo, Department of Ultrasound, Eastern Hepatobiliary Surgery Hospital, No. 225 Changhai Road, Yangpu District, Shanghai 200438, China (e-mail: jia\_guo@163.com).

Copyright © 2019 the Author(s). Published by Wolters Kluwer Health, Inc. This is an open access article distributed under the terms of the Creative Commons Attribution-Non Commercial-No Derivatives License 4.0 (CCBY-NC-ND), where it is permissible to download and share the work provided it is properly cited. The work cannot be changed in any way or used commercially without permission from the journal.

Medicine (2019) 98:31(e16533)

Received: 4 April 2018 / Received in final form: 31 May 2019 / Accepted: 27 June 2019

<http://dx.doi.org/10.1097/MD.00000000000016533>

curve [abnormal signal] to the area under the red curve [normal signal]) can be calculated with certain software, after setting the ROIs, to evaluate the degree of hepatic fibrosis quantitatively. However, the accuracy of the newly developed ASQ in diagnosing, and particularly, in grading hepatic fibrosis, has been debated.<sup>[8,10–13]</sup>

In this study, we sought to explore the practical value of ultrasonic ASQ for assessing the stages of hepatic fibrosis by comparing the ultrasonographic features of ROIs on ASQ images with the pathological characteristics of chronic viral hepatitis B patients.

## 2. Patients and methods

### 2.1. Patients

Ninety-seven patients with chronic hepatitis underwent ultrasound examination at the Ultrasound Room of Dongfang Hepatobiliary Surgery Hospital (Shanghai, China) between July 2012 and October 2013. These included 83 cases with hepatic fibrosis (71 males, and 12 females; mean age:  $50.6 \pm 10.4$  [range 17–71] years) and 14 cases with no hepatic fibrosis (9 males and 5 females; mean age:  $51.5 \pm 13.8$  [range 24–72] years). Chronic hepatitis B was diagnosed according to the 2010 Guidelines on the Prevention and Treatment of Chronic Hepatitis B. A patient was excluded from the study

- 1) if he or she had other hepatotropic virus infections;
- 2) if he or she had cholestatic liver disease, autoimmune liver disease, or alcoholic liver disease, or fatty liver. All diagnoses were confirmed pathologically.

The study protocol was approved by the Ethics Committee of our hospital. Each patient signed informed consent for study participation. The study was carried out in accordance with the tenets of the Declaration of Helsinki.

### 2.2. Approaches and methods

A color diagnostic ultrasound system (Aplio500) with a THI 5.0-MHz transducer (TOSHIBA, Minato, Japan) was used. The image depth was  $\leq 6$  cm and storage time was 3 to 4 seconds. Obvious blood vessels, bile ducts, and the shadow of the ribs were excluded from the ROI.

Patients were placed in the supine position with their legs slightly bent and arms relaxed and were asked to breathe normally. The ultrasound probe was first placed under the xiphoid; when the left lobe was ready for ASQ analysis, the ASQ interface was started. The probe was moved to the right intercostal spaces. Thereafter, patients were placed in the left lateral position, and the probe was placed below the margin of the right rib to obtain sectional images of regions V, VI, VII, and VIII of the liver, respectively. Four images of these liver sections were obtained for each patient.

After ultrasound examination, images were transferred to a computer for ASQ analysis. The ROI for ASQ was set as large as possible and was no smaller than  $30 \times 20$  mm. Hepatic tumors, large blood vessels, and bile ducts were excluded from the ROI. Each sectional image was divided into 20 to 30 sub-images, and in each sub-image, the following 6 parameters were analyzed:

- 1) red line is shown in mode 1, average 1, and SD 1;
- 2) blue line is shown in mode 2, average 2 and SD 2;
- 3)  $\text{cm}^2$ : variance of data obtained from examination/variance of healthy liver;

- 4) mode: the  $\text{cm}^2$  value of sampling points in the ROI, which showed the highest frequency;
- 5) average: the average  $\text{cm}^2$  of all sampling points in the ROI;
- 6) SD: the dispersion degree of sampling points in the ROI.

The frequency histogram of  $\text{cm}^2$  was drawn with the average on the horizontal axis and  $\text{cm}^2$  on the vertical axis.

ASQ images were analyzed by 2 similarly experienced radiologists with more 6 years of experience, who were blinded to patient information.

### 2.3. Stages of hepatic fibrosis/cirrhosis and hepatic function tests

Serum levels of aspartate aminotransferase (AST), alanine aminotransferase (ALT), and glutamyl transferase were determined as routine hepatic function test. Hepatic fibrosis was pathologically categorized into 5 stages as previously described:<sup>[14]</sup> F0 (no hepatic fibrosis), F1 (portal fibrosis), F2 (periportal fibrosis), F3 (septal fibrosis), and F4 (cirrhosis).

### 2.4. Statistical analysis

Data were analyzed with SPSF13.0, SAS9.3, and R2.15 statistical packages. Data were compared among multiple groups using univariate analysis of variance (ANOVA), followed by the Student–Newman–Keuls test if the data distribution was normal, or by the Kruskal–Wallis test if the data did not follow a normal distribution. Comparison of countable data between 2 groups was performed using Fisher exact method. Multiple stages of pathological fibrosis were compared using principal component analysis (PCA) and multivariate analysis of variance (MANOVA). If statistically significant differences were detected, the least squares difference-test or Nemenyiya test was used for further comparisons between any 2 groups. The significance level was set as 0.05. The area under the curve, sensitivity, and specificity were determined by drawing the receiver operating characteristic (ROC) curve. The cutoff was set as the value corresponding to the maximum sensitivity and specificity and used to evaluate accuracy. The ROC curve with 95% confidence interval (CI) was plotted to obtain the area under the ROC curve (AUROC), and AUROC was then used to evaluate the critical values for diagnosing fibrosis: F0 versus F1–F4 ( $\geq F1$ ); F0–F1 versus F2–F4 ( $\geq F2$ ); F0–F2 versus F3–F4 ( $\geq F3$ ), and F0–F3 versus F4 ( $\geq F4$ ). In addition, sensitivity, specificity, and accuracy were determined. Differences were considered statistically significant when  $P < .05$ .

## 3. Results

### 3.1. General characteristics of patients

Among the 97 patients, 14, 12, 34, 27, and 10 patients had stage F0, F1, F2, F3, and F4 hepatic fibrosis, respectively. There was no significant difference in demographic and baseline variables among patients with different stages of hepatic fibrosis, except for serum AST, ALT, and  $\gamma$ -glutamyl transferase levels (Table 1).

### 3.2. Direct comparison between 2-dimensional and ASQ images

The 2-dimensional acoustic images (Figure 1 A1, B1, C1, D1, and E1, <http://links.lww.com/MD/D133>) revealed increasing echo

**Table 1**  
Demographic and baseline variables of the study population\*

Variables	F0, n=14	F1, n=12	F2, n=34	F3, n=27	F4, n=10	P
Male, n (%)	9 (64.3)	10 (83.3)	28 (82.3)	23 (85.2)	10 (100.0)	.276
Age, (yr),	51.5 (42, 63)	49 (44.5, 58)	48 (44, 58)	54 (47, 59)	47.5 (40, 61)	.887
BMI (kg/m <sup>2</sup> ), mean±sd.	24.15±3.17	22.61±1.79	23.55±3.10	22.75±2.89	25.9±2.54	.065
Total bilirubin, IU/L	10.1 (9, 12.9)	14.3 (9.7, 16.5)	13.5 (10.2, 18.7)	12.7 (9.3, 16)	14 (10.8, 15.3)	.537
γ-glutamyltransferase, IU/L	34.0 (19.0, 60.0)	50.5 (34.5, 75.5)	52.5 (34.0, 75.0)	49 (23.0, 99.0)	120 (49.0, 147.0) <sup>a</sup>	.049
Alanine aminotransferase, IU/L	22 (19, 40)	23 (15.5, 28)	29 (20, 65)	36 (27, 47) <sup>a</sup>	52 (32, 64) <sup>ab</sup>	.004
Aspartate aminotransferase, IU/L	20 (18, 30)	30.5 (20.5, 44) <sup>a</sup>	32 (26, 46) <sup>a</sup>	33 (27, 42) <sup>a</sup>	35 (25, 84) <sup>a</sup>	.018
Hyaluronic acid, IU/L	88.3 (72.1, 122.7)	59.8 (50.9, 64.7)	72.2 (54.3, 83.8)	78.4 (51.7, 91.6)	128.9 (52.4, 353.8)	.324

<sup>a</sup> =  $P < .05$  compared with F<sub>0</sub>; <sup>b</sup> =  $P < .05$  compared with F<sub>1</sub>.

\* Data are expressed as median (IQR) unless otherwise indicated.

signal intensity with advancement of hepatic fibrosis from F0 to F4. However, the echo signals could not be qualitatively analyzed. ASQ color maps showed a predominantly homogeneous area under the red line for F0 (Figure 1A2, <http://links.lww.com/MD/D133>), a small area under the blue line for F1–F2 (Figure 1B2 and C2, <http://links.lww.com/MD/D133>), and a greater area under the blue line for F3–F4 (Figure 1D2 and E2, <http://links.lww.com/MD/D133>).

### 3.3. Comparison of mean cm<sup>2</sup> at different hepatic fibrosis stages

With some exceptions, there were significant differences in the mean cm<sup>2</sup> values among different stages of hepatic fibrosis in the 4 liver sections (the right lobe below the first rib, the right lobe below the second rib, the right lobe between the ribs, and the left lobe) (Table 2). Notably, no significant difference was observed in the mean cm<sup>2</sup> values between sections in the same stage (Table 2).

### 3.4. Correlation between pathological scores and stages of hepatic fibrosis detected with ASQ

Typical pathological images showing the stages of hepatic fibrosis by hematoxylin and eosin staining could be found in Supplementary Figure 1. We analyzed the correlation between hepatic fibrosis stages and mean cm<sup>2</sup> values of each image using Spearman's rank correlation test. Significant positive correlation

coefficients (R) ranged from 0.53 to 0.81, all with  $P < .01$  (Fig. 2). There were significant differences among the 5 stages (F0–F4) with PCA (Fig. 3). More importantly, multivariate analysis between ASQ cm<sup>2</sup> and different pathological stages of hepatic fibrosis revealed significant differences between any 2 adjacent stages ( $P = .03$  for F0 vs F1;  $P < .01$  for others) (Tables 3–7).

### 3.5. Determination of AUC and hepatic fibrosis stages

The averages of 4 liver sections showed no significant difference ( $P = .13$ ) with block variance analysis (data not shown). Therefore, the mean cm<sup>2</sup> of the section of the right lobe below the rib was selected as the basis for evaluating the stages of hepatic fibrosis. ROC curves were then drawn to predict the threshold values of stages in each group. The AUC reached the maximal values for F0 versus F1–F4, showing 0.969 for cm<sup>2</sup> average 1 and cm<sup>2</sup> 0.917 for average 2. However, for the comparison of F0–F3 versus F4, sensitivity reached 100% for both averages, while specificity was below 0.75 (Table 8).

## 4. Discussion

ASQ is a new technique that can be used for diagnosis of diffuse liver diseases utilizing chi-square tests. Based on the images obtained from routine ultrasonography, cm<sup>2</sup>, including mode, average, SD, and the RB ratio, can be calculated with a software after setting the ROIs. In this way, we diagnosed hepatic fibrosis quantitatively through ultrasonic examination and compared this with pathological examination.

**Table 2**  
cm<sup>2</sup> of the liver at different pathological stages of fibrosis\*

Sections		F0, n=14	F1, n=12	F2, n=34	F3, n=27	F4, n=10	P
Right lobe below rib 1	1	107.79±2.49	112.67±3.65 <sup>a</sup>	116.65±4.11 <sup>ab</sup>	124.3±7.22 <sup>abc</sup>	123.8±3.12 <sup>abc</sup>	<.001
	2	127.36±3.89	129.08±7.14	141.44±8.55 <sup>ab</sup>	146.74±6.56 <sup>abc</sup>	152.8±4.54 <sup>abcd</sup>	<.001
Right lobe below rib 2	1	109.14±4.55	114.83±3.59 <sup>a</sup>	117.71±4.49 <sup>a</sup>	123.78±7.88 <sup>abc</sup>	128.6±4.74 <sup>abcd</sup>	<.001
	2	127.86±2.98	131.08±6.04	142.94±6.95 <sup>ab</sup>	146.89±8.27 <sup>abc</sup>	155.9±6.9 <sup>abcd</sup>	<.001
Right lobe between ribs	1	108±3.51	114.17±4.45 <sup>a</sup>	116.85±4.36 <sup>a</sup>	125.11±7.59 <sup>abc</sup>	125.4±7.71 <sup>abc</sup>	<.001
	2	127.86±6.53	128.00±7.03	138.38±7.84 <sup>ab</sup>	147.52±9.27 <sup>abc</sup>	155.1±12.53 <sup>abcd</sup>	<.001
Left lobe	1	109.43±2.41	116.25±3.44 <sup>a</sup>	117.41±3.41 <sup>a</sup>	123.56±6.14 <sup>abc</sup>	122.8±3.71 <sup>abc</sup>	<.001
	2	126.64±4.53	128.58±4.27	147.65±9.74 <sup>ab</sup>	152.67±8.67 <sup>ab</sup>	153.8±5.51 <sup>ab</sup>	<.001

<sup>a</sup> =  $P < .05$  compared with F<sub>0</sub>; <sup>b</sup> =  $P < .05$  compared with F<sub>1</sub>; <sup>c</sup> =  $P < .05$  compared with F<sub>2</sub>; <sup>d</sup> =  $P < .05$  compared with F<sub>3</sub>.

\* Data are expressed as mean±SD.



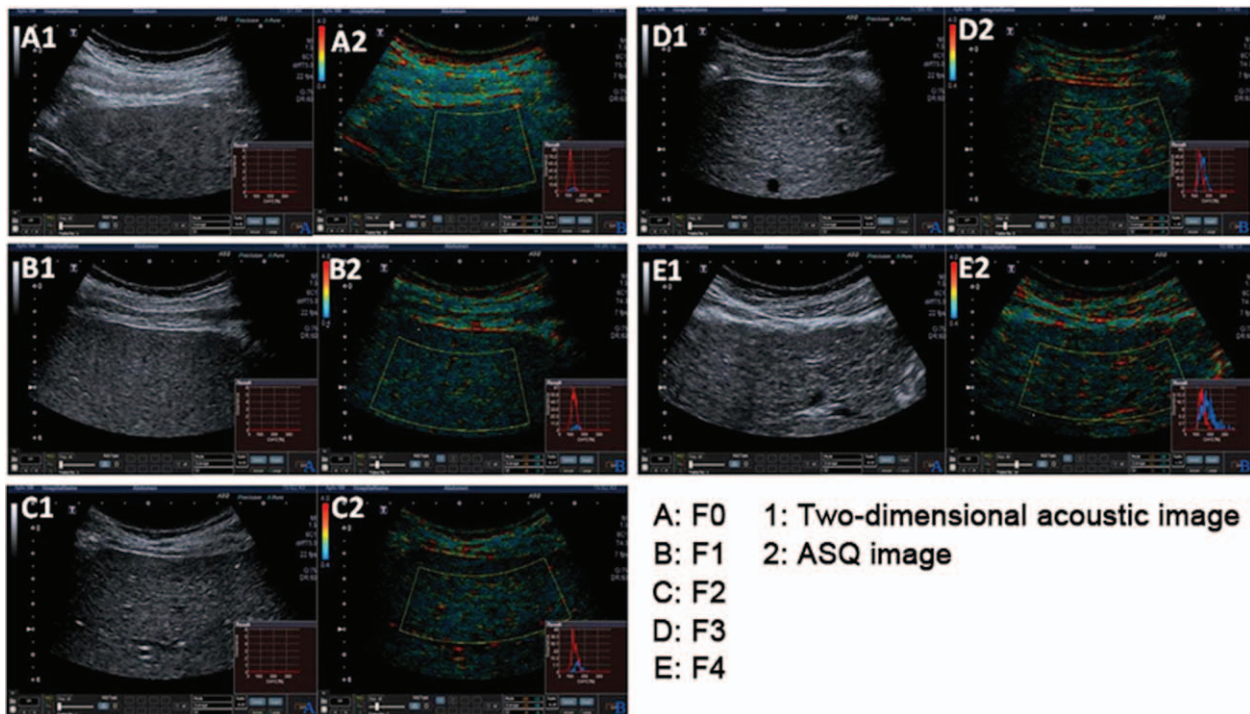


**Figure 1.** Two-dimensional acoustic images and ASQ images reveal hepatic fibrosis at different stages. ASQ=acoustic structure quantification.

We found a significant positive correlation between the mean  $\text{cm}^2$  and pathological hepatic fibrosis stages ( $P < .01$ , Fig. 2), which revealed that the mean  $\text{cm}^2$  increased with the progression of hepatic fibrosis. Furthermore, the test also indicated the highest correlation with the right liver lobe below the rib ( $r = 0.81$ ) and the lowest correlation with the left lobe ( $r = 0.59$ ). Therefore, we speculated that the data from the right lobe below the rib are more reliable than data from the left lobe, for predicting the severity of hepatic fibrosis.

In this study, there were multiple hepatic cutting surfaces (or sections), and at least 2 values (average 1 and 2) were measured for each surface. Thus, multiple parameters were obtained, and multivariate analysis was needed. PCA can analyze the main determinants from multiple parameters, thereby simplifying complex issues. In this study, the 4 pairs of mean  $\text{cm}^2$  values were analyzed using PCA and differences across all cases of fibrosis were represented using a 2-dimensional scatter plot. This plot revealed that there were statistically significant differences between any 2 groups; this was further confirmed by MANOVA. Various statistical analyses (Wilks' Lambda, Pillai's Trace, Hotelling-Lawley Trace, and Roy's Greatest Root) showed significant differences among the groups (F0-F4,  $P < .01$ , Table 3).

Next, comparisons of 2 adjacent staging groups revealed that the different pathological stages of hepatic fibrosis differed statistically significantly between 2 adjacent stages ( $P = .03$  for F0 vs F1;  $P < .01$  for the rest; Tables 4-7). A previous investigation of ASQ combined with pathological diagnosis in 148 hepatitis patients reported statistically significant differences among F0-F1 versus F2, F0-F1 versus F3 and F2 versus F3<sup>[15]</sup>, which is consistent with the results of the present study. However, Ricci

et al performed both ASQ and FibroScan on 77 patients with hepatitis B or C and 20 healthy volunteers.<sup>[13]</sup> They found no statistically significant differences between these 2 methods, and concluded that ASQ was a promising new ultrasound software program that held promise for the diagnosis of both liver cirrhosis (F = 4) and fibrosis (F  $\geq$  1).

The ROC curve presents a number of different thresholds for continuous variables by which a series of sensitivity and specificity values can be derived. It further presents sensitivity as the ordinate and 1-specificity as the abscissa for drawing a curve. The AUROC range from 0.5 to 1, where 0.5 represents a completely worthless diagnosis, and 1 is the ideal. Thus, a value of 0.5 to 0.7 is thought to be of low diagnostic value, 0.7 to 0.9 represents a medium value, and a value above 0.9 represents high diagnostic value. The larger the AUROC is, the higher the diagnostic accuracy is. The Youden index is calculated from the formula: sensitivity+ specificity-1. Critical values are obtained by maximizing the Youden index. Using an ROC curve, criteria can be computed to predict the degree of hepatic fibrosis. However, in Table 8, we show that the maximal AUC (0.969) was obtained for  $\text{cm}^2$  average 1 for F0 versus F1-F4 groups, using a low criterion (110), while the maximal criterion (145) was obtained with  $\text{cm}^2$  average 2 for F0-F3 versus F4 groups, with a relatively small AUC (0.882). This indicates that a larger sample should be investigated and that the methodology should be improved in future. In addition, we did not perform sample size calculation, which should be addressed in future studies.

Despite the limitations mentioned above, which may influence the accuracy of a minor fraction of cases, ASQ has the advantage of repeatability, objective reflection of hepatic fibrosis degree, and non-invasiveness.

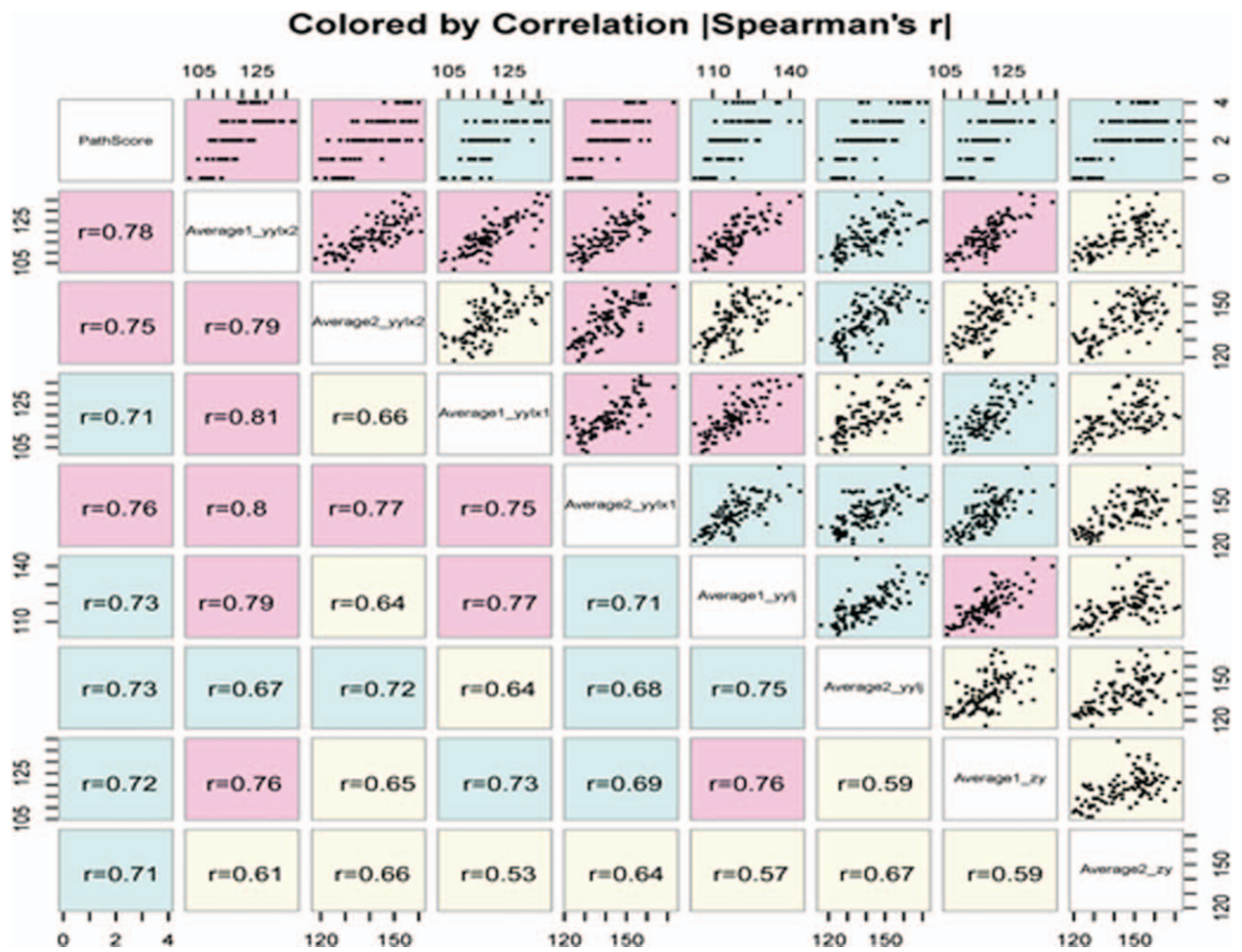


Figure 2. Spearman's correlation coefficient matrix shows correlation between the pathological scores and the cm<sup>2</sup> values of averages obtained from ASQ. Pink: the high tertile relevance (0.76–0.81); blue: mid tertile relevance (0.68–0.75); yellow: the low tertile relevance (0.53–0.67). ASQ=acoustic structure quantification.

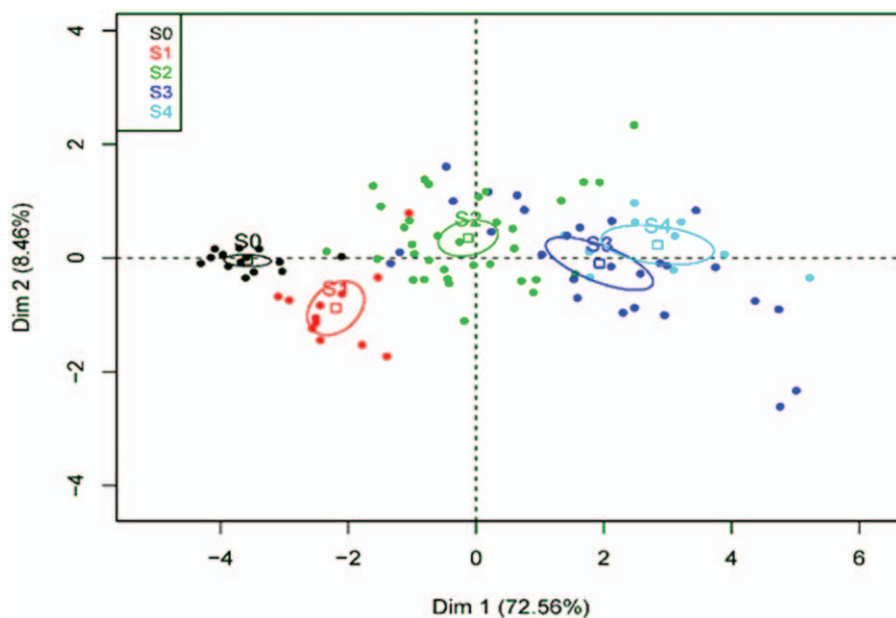


Figure 3. Scatter diagram of ASQ cm<sup>2</sup> values for different pathological stages of hepatic fibrosis according to PCA. ASQ=Acoustic Structure Quantification, PCA=principal components analysis.

**Table 3****MANOVA test criteria and F approximations for the hypothesis of no overall pathol score effect.**

Statistic	Value	F Value	Num DF	Den DF	Pr >F
Wilks' Lambda	0.10578	8.26	32	315.06	<.0001
Pillai's Trace	1.38662	5.84	32	352	<.0001
Hotelling-Lawley Trace	4.51209	11.81	32	211.85	<.0001
Roy's Greatest Root	3.67173	40.39	8	88	<.0001

H=Type III SSCP Matrix for PathScore E=Error SSCP Matrix.  
 S=4 M=1.5 N=41.5

**Table 4****MANOVA test criteria and Exact F statistics for the hypothesis of no overall F0 versus F1 effect.**

Statistic	Value	F Value	Num DF	Den DF	Pr >F
Wilks' Lambda	0.82198	2.30	8	85	0.0277
Pillai's Trace	0.17802	2.30	8	85	0.0277
Hotelling-Lawley Trace	0.21658	2.30	8	85	0.0277
Roy's Greatest Root	0.21658	2.30	8	85	0.0277

H=Contrast SSCP Matrix for F0 versus F1.  
 E=Error SSCP Matrix S=1 M=3 N=41.5

**Table 5****MANOVA test criteria and Exact F statistics for the hypothesis of no overall F1 versus F2 effect.**

Statistic	Value	F Value	Num DF	Den DF	Pr >F
Wilks' Lambda	0.52244	9.71	8	85	<.0001
Pillai's Trace	0.47756	9.71	8	85	<.0001
Hotelling-Lawley Trace	0.91411	9.71	8	85	<.0001
Roy's Greatest Root	0.91411	9.71	8	85	<.0001

H=Contrast SSCP Matrix for F1 versus F2.  
 E=Error SSCP Matrix S=1 M=3 N=41.5

**Table 6****MANOVA test criteria and Exact F statistics for the hypothesis of no overall F2 versus F3 effect.**

Statistic	Value	F Value	Num DF	Den DF	Pr >F
Wilks' Lambda	0.59678	7.18	8	85	<.0001
Pillai's Trace	0.40322	7.18	8	85	<.0001
Hotelling-Lawley Trace	0.67566	7.18	8	85	<.0001
Roy's Greatest Root	0.67566	7.18	8	85	<.0001

H=Contrast SSCP Matrix for F2 versus F3.  
 E=Error SSCP Matrix S=1 M=3 N=41.5

**Table 7****MANOVA test criteria and Exact F statistics for the hypothesis of no overall F3 versus F4 effect.**

Statistic	Value	F Value	Num DF	Den DF	Pr >F
Wilks' Lambda	0.70259	4.50	8	85	0.0001
Pillai's Trace	0.29741	4.50	8	85	0.0001
Hotelling-Lawley Trace	0.42331	4.50	8	85	0.0001
Roy's Greatest Root	0.42331	4.50	8	85	0.0001

H=Contrast SSCP Matrix for F3 versus F4.  
 E=Error SSCP Matrix S=1 M=3 N=41.5

**Table 8****Summary of ROC curve results.**

	Average	AUC	Sensitivity	Specificity	Criterion
F <sub>0</sub> vs F <sub>1</sub> -F <sub>4</sub>	1	0.969	92.8%	92.9%	110
	2	0.917	81.9%	100.0%	133
F <sub>0</sub> -F <sub>2</sub> vs F <sub>3</sub> -F <sub>4</sub>	1	0.886	78.4%	86.7%	116
	2	0.867	78.4%	76.7%	140
F <sub>0</sub> -F <sub>3</sub> vs F <sub>4</sub>	1	0.802	100.0%	64.4%	118
	2	0.882	100.0%	71.3%	145

## Author contributions

**Conceptualization:** Jia Guo.

**Formal analysis:** Yongan Chen.

**Methodology:** Lei Cheng, Rui Xiao.

**Software:** Lei Cheng, Rui Xiao.

**Validation:** Yan Pan.

**Writing – original draft:** Rui Xiao, Yan Pan.

**Writing – review & editing:** Yongan Chen, Jia Guo.

## References

- [1] Foucher J, Castera L, Bernard PH, et al. Prevalence and factors associated with failure of liver stiffness measurement using FibroScan in a prospective study of 2114 examinations. *Eur J Gastroenterol Hepatol* 2006;18:411–2.
- [2] Nel I, Lucar O, Petitdemange C, et al. Accumulation of intrahepatic TNF- $\alpha$ -producing NKp44+ NK cells correlates with liver fibrosis and viral load in chronic HCV infection. *Medicine* 2016;95:e3678.
- [3] Rizk FH, Sarhan NI, Soliman NA, et al. Heat shock protein 47 as indispensable participant in liver fibrosis: possible protective effect of lactoferrin. *IUBMB Life* 2018;70:795–805.
- [4] Zoubek ME, Trautwein C, Strnad P reversal of liver fibrosis: from fiction to reality. *Best Pract Res Clin Gastroenterol* 2017;31:129–41.
- [5] Kaneko T, Teshigawara O, Sugimoto H, et al. Signal intensity of the liver parenchyma in microbubble contrast agent in the late liver phase reflects advanced fibrosis of the liver. *Liver Int* 2005;25:288–93.
- [6] Miles KA, Hayball MP, Dixon AK Functional images of hepatic perfusion obtained with dynamic CT. *Radiology* 1993;188:405–11.
- [7] Zhang T, Li C. New advances in MRI research of hepatic fibrosis. *Radiat Pract* 2010;25:454–7.
- [8] Huang Y, Wang Z, Liao B, et al. Assessment of liver fibrosis in chronic hepatitis B using acoustic structure quantification: quantitative morphological ultrasound. *Eur Radiol* 2016;26:2344–51.
- [9] Liu J, Ren W, Ai H, et al. Acoustic structure quantification versus point shear wave speed measurement for the assessment of liver fibrosis in viral hepatitis B. *Ultrasound Med Biol* 2018;44:1177–86.
- [10] Huang Y, Liu GJ, Liao B, et al. Impact factors and the optimal parameter of acoustic structure quantification in the assessment of liver fibrosis. *Ultrasound Med Biol* 2015;41:2360–7.
- [11] Karlas T, Berger J, Garnov N, et al. Estimating steatosis and fibrosis: comparison of acoustic structure quantification with established techniques. *World J Gastroenterol* 2015;21:4894–902.
- [12] Kramer C, Jaspers N, Nierhoff D, et al. Acoustic structure quantification ultrasound software proves imprecise in assessing liver fibrosis or cirrhosis in parenchymal liver diseases. *Ultrasound Med Biol* 2014;40:2811–8.
- [13] Ricci P, Marigliano C, Cantisani V, et al. Ultrasound evaluation of liver fibrosis: preliminary experience with acoustic structure quantification (ASQ) software. *Radiol Med* 2013;118:995–1010.
- [14] Batts KP, Ludwig J. Chronic hepatitis. An update on terminology and reporting. *Am J Surg Pathol* 1995;19:1409–17.
- [15] Toyoda H, Kumada T, Kamiyama N, et al. B-mode ultrasound with algorithm based on statistical analysis of signals: evaluation of liver fibrosis in patients with chronic hepatitis C. *AJR Am J Roentgenol* 2009;193:1037–43.